J Eng Math (2007) 62:161–172
DOI 10.1007/s10665-007-9186-y

Hydraulic formulae for the added masses of an impermeable sphere moving near a plane wall

Alexander Andreevich Kharlamov · Zdeněk Chára · Pavel Vlasák

Received: 5 January 2007 / Accepted: 6 August 2007 / Published online: 7 September 2007

Abstract Simple formulae for the components of the added-mass coefficient tensor of a sphere moving near a wall with variable velocity in an ideal fluid bounded by a solid surface are derived. The added mass is calculated numerically as a function of the dimensionless distance between the sphere and the wall for both perpendicular and parallel motions. The calculation is performed by the method of successive images. The velocity field is computed as the sum of the velocity fields of sequences of dipoles located along the axis. The obtained dependences of the added-mass tensor components are fitted by simple continuous functions with high accuracy.

Keywords Added mass · Ideal fluid · Image method · Numerical solution · Sphere moving near plain wall

1 Introduction

When a sphere moves in an unbounded ideal incompressible fluid, the only effect it experiences is that it acquires additional mass equal to half of the water mass displaced by the sphere. In this case the added-mass coefficient C_m equals 0.5. The presence of a solid wall leads to an increase of the mass with a decrease of the distance to the wall. As a consequence of the added-mass dependence on the distance of the sphere to the wall, a force arises that is proportional to the square of the sphere velocity [1]. The direction of the sphere motion also affects the added mass. Thus, the added mass of a sphere in the vicinity of a solid plane is no longer a scalar quantity, but a tensor, which will be introduced below.

Knowledge of the added mass of a spherical particle is important for many engineering disciplines, for instance in river engineering, water treatment and gas-particle or liquid-particle flow in the presence of a solid surface. For the saltation mode of bed-load transport a knowledge of the added mass is important because, during saltation, the moving particles periodically collide with the bed (see [2]). It is also indispensable for a dynamical analysis of the motion of a sphere near a wall or for the numerical modelling of the motion of a sphere (see [3]).

The problem of the motion of a sphere in an ideal incompressible fluid in the vicinity of a wall can be seen as a special case of the more general problem of the motion of two spheres, provided that the velocity field in the first case is the same as that generated by the symmetric motion of two equal spheres with the wall being replaced by

A. A. Kharlamov (✉) · Z. Chára · P. Vlasák
The Institute of Hydrodynamics AS CR, v.v.i., Pod Pat'ankou 30/5, 166 12, Prague 6, Czech Republic
e-mail: charlamov@ih.cas.cz

the plane of symmetry. The problem can be split into two problems, namely, (i) the spheres moving perpendicularly and (ii) moving parallel to the line joining their centres [1].

The problem of the motion of two spheres in an ideal incompressible fluid has been addressed by many authors; see e.g. [4–14].

For distances to the wall much larger than the radius of the sphere, Stokes [4] derived approximate expressions for the fluid potential and calculated the increase of the sphere mass as a function of the distance from the centre of the sphere to the wall for the cases of parallel and perpendicular motions. He considered the motion induced by the sphere in the absence of the wall, the motion induced by the second sphere that is the mirror reflection of the first sphere in the plane of the wall, and the motion induced by the first sphere that compensates the motion of the sphere reflection. Then the three motions were superposed to obtain the result.

Hicks [5] described the image method in detail. This method permits construction of the velocity field from a sequence of dipoles. This method becomes very complicated when the spheres move perpendicularly to the line connecting their centres; however, with the development of computer engineering, it became possible to resolve the problem with sufficient accuracy. For the axisymmetric case, he calculated the fluid kinetic energy in the form of an infinite series; for a sphere contacting a wall, he calculated an added-mass coefficient equal to 0.803085. In the case when the spheres move perpendicularly to the line connecting their centres, Hicks abandoned the attempt to obtain a complete solution, and resorted to an approximate one.

Basset [6] calculated an approximate expression for the fluid potential and for the kinetic energy of a fluid for spheres moving parallel to the line connecting their centres, as well as for the case of perpendicular motion. The obtained expressions are valid only for large distances between the spheres.

Kawaguti [7] investigated the special case of the motion of two spheres passing each other to estimate the pressure variation when two high-speed trains pass each other. The problem was approximately solved numerically using the image method.

Shebalov [8] considered the motion of an arbitrary body under a solid wall. The velocity potential was calculated using the Kochin method (see [9]). For the added mass of a sphere moving parallel to a wall, he gave an expression coinciding with Stokes' result.

Voinov [10] derived expressions for the flow potential and the kinetic energy of a fluid in the form of an infinite sum in the case when spheres move perpendicularly to line joining their centres. An integral operator in the sum terms is applied repeatedly to a dipole potential. The integral operator reflects the image method described in [5]. Voinov also calculated the kinetic energy of a fluid for the case when equal spheres move in contact with equal velocities. In this case, the added-mass coefficient equals 0.621.

Weihs and Small [11] found an exact solution for the motion of two spheres in axisymmetric potential flow. They solved the Laplace equation in bispherical coordinates by means of separation of variables. The general solution in series form was then employed to calculate the added mass of a sphere approaching a wall. They plotted the result for the added mass and compared it graphically with the classical result obtained by the image method. The image-method solution approached that of Weihs and Small when the image number was increased.

Miloh [12] found an exact solution for the arbitrary motion of two spheres in an ideal incompressible fluid. The problem was formulated in terms of spherical harmonics. The fluid velocity potentials for the parallel and perpendicular motion were found as infinite sums. The derived kinetic-energy expression involved only the first terms of the sums considered. The coefficients in the sums were defined as the solution of an infinite set of linear equations. As a particular case, the motion of a sphere parallel to and perpendicular to a plane wall was considered. The plots of added masses found numerically depending on the distance to the wall were presented. The added masses at contact were reported to coincide with the previous results.

Bentwich and Miloh [13] obtained an exact solution of the motion of two spheres in axisymmetric potential flow. Their solution differs from the previous work in that the stream function is used rather than the potential function. Bispherical coordinates were used in the calculations. The solution was given in the form of an infinite series. A general expression was obtained for the kinetic energy of the system. They also calculated the added-mass coefficient for a sphere approaching a wall at an instance of contact, which coincides with the previous results.

Yang [14] studied the collision of two solid particles and the collision of a particle with a wall. For the axisymmetric case of sphere-wall collision, he estimated the added mass of the sphere using the successive-image method. He suggested cutting off the sequence of images after the seventh term. However, the formula proposed for the added mass is quite accurate only far away from the wall and yields an error of about 1.3% at contact.

The motion of two spheres in mutual contact was studied by Majumder [15], Small and Weihs [16], Morrison [17], Davis [18], Jeffrey and Chen [19], and Cox and Cooker [20]. Majumder [15] seems to be the first to examine the problem of two touching spheres in an incompressible ideal fluid. He found the stream flow function in integral form for the axisymmetric case using tangent-sphere coordinates.

Small and Weihs [16] presented an exact solution for the axisymmetric incompressible potential flow over two touching spheres. The Laplace equation was solved in tangent-sphere coordinates. They obtained a solution in the form of an infinite series for the flow potential. The added-mass expression for a sphere touching the wall was also derived. However, in contradiction to their previous results (see [11]), they concluded that the added mass in contact is infinite. Later, Morrison [17] and Jeffrey and Chen [19] pointed out that this suggestion was erroneous. Morrison [17], correcting the results of Small and Weihs [16], derived the expression for the flow potential, replacing the infinite series in the solution by an integral. Using the same method, Jeffrey and Chen [19] calculated the flow potential and the added mass, which was finite and coincided exactly with the previous results.

Using tangent-sphere coordinates, Davis [18] solved the problem of two equal spheres in contact moving perpendicularly to a line connecting their centres. The flow potential satisfying the Laplace equation was expressed as an integral over an unknown function. An ordinary differential equation satisfied by this function was solved numerically and the kinetic energy of the fluid was evaluated. Davies reported an added-mass coefficient of 0.621, which coincides with the result of Voinov [10]. Based on the method of Davis [18], Cox and Cooker [20] found the velocity potential of an ideal incompressible fluid past a sphere moving in contact with a wall. The unknown function was found numerically to a high degree of accuracy and then a detailed presentation was given of the potential near the sphere. The added-mass coefficient was found to be equal to 0.621, confirming previous results.

Many papers have been written on the added masses of a sphere in the vicinity of a wall. Most of the solutions are in the form of infinite series or integrals. The presented expressions are too complicated to be used in fluid-mechanics problems and additional calculations are required before their introduction becomes possible. Only Yang [14], for the axisymmetric case, presented a simple formula for added-mass coefficient $C_m^{\perp}$ versus distance to the wall h, although the accuracy close to the contact point is reduced and, on the other hand, when the accuracy is increased, the formula becomes too cumbersome. To the best of the authors' knowledge, there is still no useful expression for the added-mass coefficient of a sphere moving parallel to a wall $C_m^{\parallel}$ at any distance from the wall. The task seems to be intractable analytically, but readily solvable numerically. The present paper yields formulae for $C_m^{\perp}$ and $C_m^{\parallel}$ that are not bulky and are valid with high accuracy for all distances from the wall.

The mathematical model, based on the image method, for the construction of the velocity potential and calculation of the added-mass coefficients in both parallel and perpendicular cases is described in Sect. 2. The results of a numerical calculation are described in Sect. 3. The calculated added-mass coefficients are reported as functions of the dimensionless distance between the centre of the moving sphere and the wall, and the achieved accuracy is estimated.

2 Mathematical model

Usually, the dimensionless added-mass coefficient C_m is introduced as ([2,21]):

$$\vec{F}_m = -C_m \Omega \rho_f \frac{\mathrm{d}\vec{u}}{\mathrm{d}t}, \tag{1}$$

where $\vec{F}_m$ is the added-mass force, Ω is the sphere volume, ρ_f is the fluid density and $\vec{u}$ is the sphere velocity. In an unbounded fluid, $C_m = 0.5$.

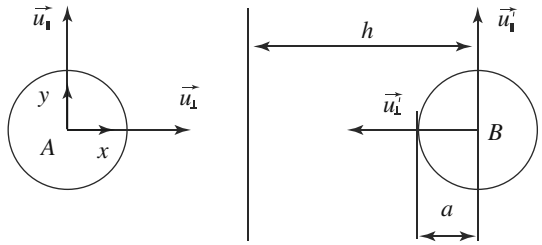

Fig. 1 Motion of a sphere parallel and perpendicular to the wall

In potential-flow theory, the added-mass coefficient is calculated from the kinetic energy of the fluid. In an unbounded fluid, the kinetic energy is expressed as (see [1])

$$2T = \frac{2}{3}\pi\rho_f a^3 u^2 = M' u^2, \tag{2}$$

where a is the sphere radius and M' is the virtual increment of the sphere mass. In terms of the dimensionless added-mass coefficient, one has

$$2T = C_m \Omega \rho_f u^2. \tag{3}$$

In the presence of the wall, the motion of the sphere can be considered to be the sum of two motions, perpendicular to the wall and parallel to the wall. The kinetic energy of a fluid for arbitrary motion of the sphere is equal to the fluid energies for these sphere motions:

$$2T = M'_\parallel u_\parallel^2 + M'_\perp u_\perp^2, \tag{4}$$

or, defining the x-axis perpendicular to the wall, for the most common motion, we can write

$$2T = M'_\perp u_x^2 + M'_\parallel u_y^2 + M'_\parallel u_z^2 = (C_m^\perp u_x^2 + C_m^\parallel u_y^2 + C_m^\parallel u_z^2)\Omega\rho_f. \tag{5}$$

Writing the last expression in tensor form yields

$$\frac{2T}{\Omega\rho_f} = C_m^{ij} u_i u_j, \tag{6}$$

where the summation is implied over i, j, and the added-mass-coefficient tensor C_m^{ij} is introduced. In a special coordinate system, where the x-axis is perpendicular to the wall, C_m^{ij} is diagonal and has only two essential components $C_m^\parallel$ and $C_m^\perp$. Thus, it is sufficient to calculate the kinetic energy for two cases, namely when the sphere moves parallel to and perpendicularly to the wall (see [1]). Let us consider two equal spheres A and B (the centres of the spheres are denoted by the same symbols) moving symmetrically at velocities with equal absolute values $u = u'$. Let the xy-plane be the plane of motion and A the coordinate origin; see Fig. 1.

2.1 Motion perpendicular to the wall

Following the standard procedure, we can write the fluid velocity potential in the form

$$u_\perp \varphi + u'_\perp \varphi', \tag{7}$$

where functions φ and φ' are to be determined by the conditions

$$\Delta\varphi = 0, \quad \Delta\varphi' = 0, \tag{8}$$

and boundary conditions such that φ is the value of the velocity potential when sphere A moves with unit velocity along the spheres centres line while sphere B is at the rest; and similarly for φ'.

To find φ (if sphere B is absent), we assume that the motion of the fluid will be due to a certain dipole at point A with its axis co-directed with the sphere velocity vector. If we introduce an image in sphere B of the dipole

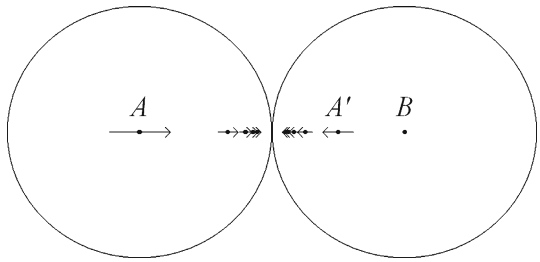

Fig. 2 The consequence of the dipoles when sphere A moves in contact with sphere B, which is at rest. The dipoles are denoted by arrows. The length of an arrow is proportional to the cubic root of the dipole strength

existing at point A, the condition of zero normal velocity over the surface of sphere B will be satisfied (see [5]). The resultant motion due to the dipole and the first image will, however, violate this condition at the surface of sphere A. In order to neutralize the normal velocity at the surface of sphere A, due to the first image, we must superimpose a second image, namely the image of the first image in sphere A. This will introduce a normal velocity at the surface of sphere B, which may again be neutralized by adding another image and so on.

The velocity potential generated by the initial dipole in a point with position vector $\vec{r}(x, y, z)$ will be

$$\varphi_1 = -\frac{\mu_1}{4\pi}\frac{x}{|\vec{r}|^3} = -\frac{\mu_1}{4\pi}\frac{\cos\vartheta}{|\vec{r}|^2}, \tag{9}$$

where $\mu_1 = 2\pi a^3$ is the strength of the dipole, ϑ is the angle between the dipole direction and vector from the dipole to the point considered. The image of the initial dipole consists of a dipole of opposite sign at the inverse point A' determined by

$$AB \cdot A'B = a^2. \tag{10}$$

The strength of the image dipole is

$$\mu_2 = -\mu_1 \frac{a^3}{AB^3}. \tag{11}$$

The next images are allocated similarly according to the aforementioned procedure. The coordinates of the dipoles compose a sequence of inverse points. From coordinate x_i and strength μ_i of the ith dipole, coordinate x_{i+1} and strength μ_{i+1} of the $(i+1)$th dipole can be determined as follows:

$$x_{i+1} = x_{AB} - \frac{a^2}{x_{AB} - x_i}, \tag{12}$$

$$\mu_{i+1} = -\mu_i \frac{a^3}{|x_{AB} - x_i|^3}, \tag{13}$$

where $x_{AB} = x_A = 0$ if i is even and $x_{AB} = x_B$ otherwise. When the spheres are in contact ($x_B = 2a$), the distance from the successive ith dipole to the point of contact is inversely proportional to the dipole number; see Fig. 2. The images continually diminish in intensity, and the series converges very rapidly at high distances and rather slowly at small distances between the spheres. The same steps are used to calculate the velocity-potential φ', provided that the coordinates of the moving and immobile spheres are exchanged and the strength of the first dipole changes sign.

The formula for the kinetic energy of the fluid is

$$2T = -\rho_f \iint_{A,B} (u_\perp \varphi + u'_\perp \varphi') \left(u_\perp \frac{\partial \varphi}{\partial n} + u'_\perp \frac{\partial \varphi'}{\partial n} \right) \mathrm{d}s = L u_\perp^2 + 2M u_\perp u'_\perp + N u'^2_\perp, \tag{14}$$

where integration is effected over both the sphere surfaces and $\vec{n}$ is the normal to the surface unit vector. According to [5], the following formulae are valid for L, M, and N:

$$L = \frac{1}{3}\rho_f(\mu_1 + 3\mu_3 + 3\mu_5 + \cdots), \tag{15}$$

$$M = \rho_f(\mu'_2 + \mu'_4 + \mu'_6 + \cdots), \tag{16}$$

$$N = -\frac{1}{3}\rho_f(\mu'_1 + 3\mu'_3 + 3\mu'_5 + \cdots). \tag{17}$$

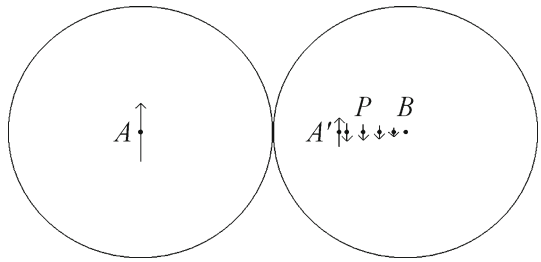

Fig. 3 The image in sphere B of the first dipole in A. The image consists of the dipole in inverse point A' and of the line dipole distribution approximated by four dipoles. The dipoles are denoted by arrows with lengths proportional to the cubic root of the dipole strength

Primes mark values corresponding to the dipoles that generate the potential φ'. Thus, in this case, it is sufficient to employ simple summation. The component of the added-mass-coefficient tensor is determined from the kinetic energy of a fluid, viz,

$$2T = 2\Omega\rho_f C_m^{\perp} u_{\perp}^2. \tag{18}$$

The factor two in the right-hand side of Eq. 18 arises from the fact that, on the left-hand side, the energy corresponds to the entire infinite space, and we are interested in the energy of fluid in semi-space.

2.2 Motion parallel to the wall

When the spheres move perpendicularly to the line connecting their centres, potentials φ and φ' are defined in a similar manner as in the previous section. Potential φ is approximated as the potential of a series of successive images starting from the initial dipole. The initial dipole is located at point A with its axis directed perpendicularly to the line joining the centres of the spheres. The image of the initial dipole consists of a dipole of the same sign at the inverse point in sphere B and a line dipole distribution of opposite sign with linear density on the segment connecting point B and the inverse point A'; see Fig. 3 for the case of touching spheres. The dipole strength at the inverse point is:

$$\mu_2 = \mu_1 \frac{a^3}{AB^3}, \tag{19}$$

The density of the line dipole distribution is

$$\tilde{\mu}_2(P) = -\frac{\mu_1}{a}\frac{BP}{AB}, \tag{20}$$

where P is a point of segment $A'B$.

For the calculation, the line distribution of the dipoles was approximated by m dipoles. Segment $A'B$ was split into m equal sub-segments and, on each sub-segment, a dipole was located at the equilibrium point of the sub-segment. The strength of the dipole equalled the integral strength of the dipole distribution of the corresponding sub-segment. The "equilibrium point" means the point with coordinate x_{eq}^j determined by

$$\int_{x_b^j}^{x_{\mathrm{eq}}^j} \tilde{\mu}(x)\mathrm{d}x = \int_{x_{\mathrm{eq}}^j}^{x_b^{j+1}} \tilde{\mu}(x)\mathrm{d}x, \tag{21}$$

where x_b^j and x_b^{j+1} are the coordinates of the edges of the jth sub-segment.

The approximation of the dipole distribution by several dipoles allows a determination of the second image as a sum of the images of each of the dipoles comprising the first image. The third image will be the sum of the images of all the dipoles comprising the second image and so on. The image of the ith dipole with coordinate x_i and strength μ_i will be the $(i+1)$th dipole in the inverse point, see Eq. 12, with strength

$$\mu_{i+1} = \mu_i \frac{a^3}{|x_{AB} - x_i|^3}, \tag{22}$$

and m dipoles with strengths

$$\mu_{i+1}^{j} = -\mu_i \frac{a^3}{|x_{AB} - x_i|^3} \frac{j + 0.5}{m^2} \tag{23}$$

and coordinates

$$x_{i+1}^{j} = x_{AB} + \frac{a^2}{m(x_i - x_{AB})} \sqrt{j^2 + j + 0.5}, \quad 0 \le j \le m - 1, \tag{24}$$

where $x_{AB} = x_A = 0$ if the ith dipole is in sphere B and $x_{AB} = x_B$ otherwise.

The first image consists of $m + 1$ dipoles; the second image consists of $(m + 1)^2$ dipoles. If we approximate potential φ by n images, we must consider

$$1 + (m + 1) + (m + 2)^2 + \cdots + (m + 1)^n = \frac{(m + 1)^{n+1} - 1}{m} \tag{25}$$

dipoles and the same number for ϕ'. According to [10], the kinetic-energy expression formed by an infinite series corresponding to an infinite sequence of images converges faster when the spheres move perpendicularly to the line joining their centres, than when they move parallel to this line; thus, fewer images are needed to achieve the same accuracy. In the next section, parameters m and n, and accuracy will be discussed.

The integral for the kinetic energy over the sphere surface can be taken analytically for each dipole, thus representing the kinetic energy as a sum. Due to the symmetry of the problem, the integral over sphere A is equal to the integral over sphere B. Taking into account the boundary condition on the sphere surface $u_{\parallel} \frac{\partial \varphi}{\partial n} + u'_{\parallel} \frac{\partial \varphi'}{\partial n} = \vec{u}_{\parallel} \vec{n}$, and bearing in mind that the flow potential is modelled by a finite set of dipoles φ_i, we can write

$$2T = -2\rho_f u_{\parallel}^2 \oiint_A (\varphi + \varphi') \frac{\partial(\varphi + \varphi')}{\partial n} \mathrm{d}s = -2\rho_f u_{\parallel} \sum_{m,n} \oiint_A \varphi_i \vec{u}_{\parallel} \vec{n} \mathrm{d}s = -2\rho_f u_{\parallel} \sum_{m,n} I_i, \tag{26}$$

where the summation is carried out over all the model dipoles. The integral equals

$$\begin{aligned} I_i &= \int_0^{\pi} \int_0^{2\pi} \left(-\frac{\mu_i}{4\pi} \frac{y}{|\vec{r} - \vec{r}_i|^3} \right) (u_{\parallel} \sin\vartheta \cos\alpha) a^2 \sin\vartheta \mathrm{d}\alpha \, \mathrm{d}\vartheta \\ &= -\frac{\mu_i u_{\parallel}}{4\pi} \int_0^{\pi} \int_0^{2\pi} \frac{a^3 \sin^3\vartheta \cos^2\alpha}{(a^2 - 2x_i a \cos\vartheta + x_i^2)^{3/2}} \mathrm{d}\alpha \mathrm{d}\vartheta = \begin{cases} \dfrac{\mu_i u_{\parallel}}{3}, & |x_i| < a \\ \dfrac{\mu_i u_{\parallel}}{3} \dfrac{a^3}{x_i^3}, & |x_i| > a \end{cases} \end{aligned} \tag{27}$$

Here α is an azimuthal angle, x_i and μ_i are the x-coordinate and the strength of the ith dipole, respectively. Component $C_m^{\parallel}$ of the added-mass-coefficient tensor can now be calculated from

$$2T = 2\Omega\rho_f C_m^{\parallel} u_{\parallel}^2. \tag{28}$$

3 Results

In the axisymmetric case, the added-mass coefficient was calculated numerically using Eqs. 14–18. To achieve a precision of six significant figures after the decimal point, it was sufficient to construct 1000 symmetric pairs of dipoles for the contact of the spheres. The added mass $C_m^{\perp}$ at contact is 0.803085, which agrees with previous results.

The added-mass coefficient $C_m^{\perp}$ was calculated for 200 sphere positions with dimensionless distances of the sphere centre from the wall $\bar{h} = \frac{h}{a}$ between 15 and 1 with increasing position density close to the point of contact. The calculated data were fitted using a least-squares method with the following function and with maximum deviation from the computed data 8×10^{-5}:

$$C_m^{\perp} = 0.5 + H_1 \bar{h}^{t_1} + H_2 \bar{h}^{t_2} + H_3 \bar{h}^{t_3} + H_4 \bar{h}^{t_4}, \tag{29}$$

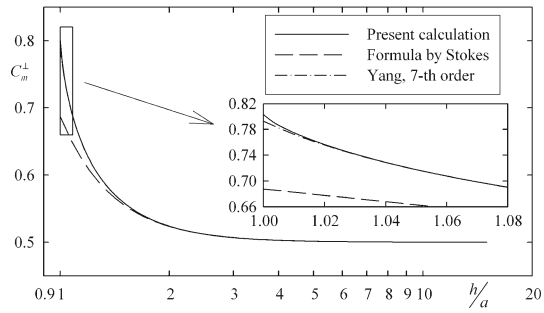

Fig. 4 Added-mass coefficient $C_m^\perp$ of a sphere for velocity vector perpendicular to the wall

where

$$\begin{aligned} H_1 &= 0.19222, \quad t_1 = -3.019, \\ H_2 &= 0.06214, \quad t_2 = -8.331, \\ H_3 &= 0.0348, \quad t_3 = -24.65, \\ H_4 &= 0.0139, \quad t_4 = -120.7. \end{aligned} \tag{30}$$

For the cases when such high accuracy is not required, another, more simple formula can be used, yielding a deviation of maximum 4×10^{-3}:

$$C_m^\perp = 0.5 + H_1' \bar{h}^{t_1'} + H_2' \bar{h}^{t_2'}, \tag{31}$$

where

$$\begin{aligned} H_1' &= 0.2182, \quad t_1' = -3.21, \\ H_2' &= 0.081, \quad t_2' = -19. \end{aligned} \tag{32}$$

A plot of $C_m^\perp$ versus $\bar{h}$ is presented in Fig. 4. The result can be compared with those of Stokes [4] and Yang [14]. The Stokes result yields

$$C_m^\perp = C_m \left(1 + \frac{3}{8}\frac{1}{\bar{h}^3}\right), \tag{33}$$

and the Yang result yields

$$C_m^\perp = C_m \left(1 + 3W_7\left(\bar{h}\right)\right), \tag{34}$$

$$\begin{aligned} W_7(\bar{h}) = {} & \frac{1}{8\bar{h}^3} + \frac{1}{(4\bar{h}^2-1)^3} + \frac{1}{(8\bar{h}^3-4\bar{h})^3} + \frac{1}{(16\bar{h}^4-12\bar{h}^2+1)^3} + \frac{1}{(32\bar{h}^5-32\bar{h}^3+6\bar{h})^3} \\ & + \frac{1}{(64\bar{h}^6-80\bar{h}^4+24\bar{h}^2-1)^3} + \frac{1}{(128\bar{h}^7-192\bar{h}^5+80\bar{h}^3-8\bar{h})^3} \end{aligned} \tag{35}$$

As can be seen from Fig. 4, Eq. 33 is quite accurate for $\bar{h} \geq 2$, and Eqs. 34, 35 are quite accurate for $\bar{h} \geq 1.02$.

When a sphere moves parallel to a wall, we used Eqs. 26–28. The resultant accuracy depends on two parameters, m and n, which were defined in the previous section. To estimate the accuracy, the parameters were increased steadily and values of the added mass at contact for different combinations m, n was calculated; see Table 1. As the numbers m, n increased, the accuracy increased. Computational capabilities limit the numbers m and n. Thus, the following procedure was employed to determine the limit and the accuracy.

The Shanks method was used to estimate the limit of the convergent series [22]. The method allows acceleration of the convergence of slowly convergent series a_i by applying the nonlinear transformation:

$$b_i = \frac{a_{i+1}a_{i-1} - a_i^2}{a_{i+1} + a_{i-1} - 2a_i}. \tag{36}$$

The transformation reduces the number of elements in the series by two. If we have a limited number of series elements a_i, then, after applying a transformation according to Eq. 36 several times, we obtain a limit that is usually several orders closer to $\lim_{i\to\infty} a_i$ than any of the available a_i.

Table 1 Added-mass coefficient $C_m^{\parallel}$ at the point of contact; sphere moves parallel to the wall

$_m{}^n$	6	7	8	9	10	11
1	0.6200138508	0.6204787682	0.6207800888	0.6209874361	0.6211368211	0.6212484061
2	0.6199531947	0.6203824700	0.6206538550	0.6208363444	0.6209651049	0.6210595105
3	0.6198900929	0.6202994894	0.6205538209	0.6207218407	0.6208383509	0.6209223638
4	0.6198638366	0.6202645081	0.6205111986	0.6206726096	0.6207834252	0.6208625286
5	0.6198510971	0.6202473440	0.6204901122	0.6206480914	0.6207559168	0.6208324149
6	0.6198440794	0.6202378089	0.6204783294	0.6206343273	0.6207404140	0.6208153866
7	0.6198398375	0.6202320082	0.6204711302	0.6206258895	0.6207308840	0.6208048936
8	0.6198370896	0.6202282319	0.6204664280	0.6206203645	0.6207246310	
9	0.6198352127	0.6202256421	0.6204631949	0.6206165584	0.6207203165	
10	0.6198338760	0.6202237915	0.6204608799	0.6206138288	0.6207172183	
$_m{}^n$	12	13	14	15	16	
1	0.6213342143	0.6214017919	0.6214560797	0.6215004294	0.6215371845	
2	0.6211309228	0.6211863538	0.6212303204	0.6212658394	0.6212949887	
3	0.6209849222	0.6210327720	0.6210702111	0.6211000784	0.6211243076	
4	0.6209208428	0.6209650092	0.6209992382			
5	0.6208884543	0.6209306282				
6	0.6208700849					

Cells are filled where the computational resources allow calculation and where the data is substantial for determining of the limit and the accuracy.

Table 2 The added mass $C_m^{\parallel}$ at contact estimated by the Shanks transformations applied on rows and columns of Table 1

	$7 \le n \le 13$ $1 \le m \le 5$	$6 \le n \le 12$ $2 \le m \le 6$	$7 \le n \le 11$ $1 \le m \le 7$	$6 \le n \le 10$ $2 \le m \le 10$
Rows first	0.6210747872	0.6210392848	0.6210036714	0.6209919360
Columns first	0.6210744835	0.6210377470	0.6210037636	0.6210425919

To estimate the limit, we planned to apply the Shanks transformation first to the columns and then to the calculated row, and vice versa, first to the rows, then to the calculated column. The rectangular data areas from Table 1 were used to apply this transformation, where the transformation could be applied at least twice for each direction. The limits estimated from the data in different areas are presented in Table 2.

The average and deviation can be calculated from Table 2; thus, at contact $C_m^{\parallel} = 0.62103 \pm 0.00005$. For the calculation for other distances between the wall and the sphere, the value corresponding to $m = 4, n = 13$ was chosen reasonably, and consequently the error is 0.0001. Close to this value, the error resulting from an increase in n is close to the error caused by an increase in m; the value is close to that estimated by the Shanks transformations, and the computation time is not excessive.

The added-mass coefficient $C_m^{\parallel}$ was calculated with $m = 4, n = 13$ for 200 sphere positions for distances of the sphere centre from the wall between 15 and 1 radius, with increasing position density close to the contact. The points of the function were fitted with a maximum error of 1×10^{-4}. Thus, the following formula is valid with a maximum absolute error of 2×10^{-4}:

$$C_m^{\parallel} = 0.5 + G_1 \bar{h}^{s_1} + G_2 \bar{h}^{s_2} + G_3 \bar{h}^{s_3}, \tag{37}$$

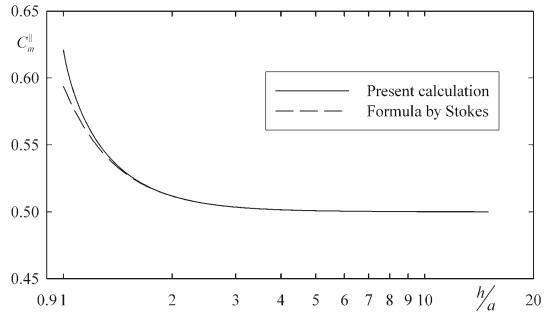

Fig. 5 Added-mass coefficient $C_m^{\parallel}$ of a sphere for velocity vector parallel to the wall

where

$$\begin{aligned} G_1 &= 0.09608, \quad s_1 = -3.02, \\ G_2 &= 0.0194, \quad s_2 = -9.6, \\ G_3 &= 0.00546, \quad s_3 = -40.2. \end{aligned} \tag{38}$$

Also we offer another, more simple formula with less accuracy, which yields an absolute error of a maximum of 8×10^{-4}:

$$C_m^{\parallel} = 0.5 + G_1' \bar{h}^{s_1'} + G_2' \bar{h}^{s_2'}, \tag{39}$$

where

$$\begin{aligned} G_1' &= 0.1, \quad s_1' = -3.1, \\ G_2' &= 0.0203, \quad s_2' = -14. \end{aligned} \tag{40}$$

The plot of $C_m^{\parallel}$ versus $\bar{h}$ is presented in Fig. 5. The result can be compared with that of Stokes [4]:

$$C_m^{\parallel} = C_m \left(1 + \frac{3}{16}\frac{1}{\bar{h}^3}\right). \tag{41}$$

As can be seen from Fig. 5, formula (41) is quite accurate for $\bar{h} \geq 2$.

According to [1], if a sphere moves in a direction perpendicular to a plane wall, the equations of motion of the sphere are:

$$\begin{aligned} &\frac{\mathrm{d}}{\mathrm{d}t}(M_{\parallel}\dot{y}) = F_y, \\ &\frac{\mathrm{d}}{\mathrm{d}t}(M_{\perp}\dot{x}) - \frac{1}{2}\left(\frac{\mathrm{d}M_{\parallel}}{\mathrm{d}x}\dot{y}^2 + \frac{\mathrm{d}M_{\perp}}{\mathrm{d}x}\dot{x}^2\right) = F_x, \end{aligned} \tag{42}$$

where x, y are the sphere-centre coordinates; in this notation x is the distance from the wall and dots above the values denote the time derivatives; F_x, F_y are the components of extraneous force on the sphere; $M_{\perp} = m_s + \rho_f \Omega C_m^{\perp}$, $M_{\parallel} = m_s + \rho_f \Omega C_m^{\parallel}$, and m_s is the sphere mass. It follows from the equations that, if the sphere is constrained to move in a line parallel to the wall, it is *attracted* by the wall; if it moves perpendicularly to the wall, its acceleration is directed *away from* the wall [1].

4 Conclusions

The problem of a potential flow of an ideal incompressible fluid past a sphere moving in the vicinity of a wall has been studied. The added-mass coefficient of the sphere can be obtained from the fluid kinetic energy. The fluid kinetic energy for arbitrary motion of a sphere equals the sum of kinetic energies for motion of the sphere parallel to and perpendicular to the wall, with velocities equal to the projections of the sphere velocity in the corresponding

directions. Thus, the problem can be solved as two problems, that is, when the sphere moves perpendicularly to the wall (axisymmetric case) and when it moves parallel to the wall. It can be expressed in tensor form with two essential components corresponding to the motion perpendicular to and parallel to the wall. The numerical approach was chosen for calculating the components, and the added-mass coefficient of the sphere moving in the vicinity of the wall was determined for both perpendicular and parallel motion of the sphere with respect to the wall.

The successive-image method was used to approximate the fluid motion. In both perpendicular and parallel cases, the fluid velocity potential was approximated as a sum of the images consisting of dipoles. For axisymmetric motion, each image consisted of one dipole; the formulae of Hicks [5] were used for the kinetic energy of the fluid. For a sphere moving parallel to the wall, the number of dipoles in each consecutive image grows as a geometric series; the integral over the sphere surface in the kinetic-energy expression was calculated for each of the model dipoles and transformed into a sum over the dipoles.

The obtained dependences of the added-mass tensor components versus the dimensionless distance to the wall were fitted with simple smooth continuous functions. Thus, simple formulae were obtained for the added-mass-coefficient tensor components.

The presented formulae for the added-mass components can be used in the problem of modelling and analysis of the motion of a sphere in a fluid near a solid wall, which can be encountered, e.g., in fluid mechanics, especially in civil and mechanical engineering.

The studied subject, i.e., added mass of a body moving in fluid near a solid surface, can be developed further by applying the used technique for calculating the energy of fluid moving past two arbitrarily moving spheres. In the case of unequal sphere radii, the coefficients in the energy expression will also depend on the ratio of the radii. If the method would turn out to be practical, even in the case of more than two bodies, the research area could be greatly extended.

Acknowledgements Support under project No. 103/06/1487 of the Grant Agency of the Czech Republic and under Institutional Research Plan No. AV0Z20600510 of the Academy of Sciences of the Czech Republic is gratefully acknowledged.

References

1. Lamb H (1951) Hydrodynamics, 6th edn. Cambridge University Press, Cambridge
2. Nino Y, Garcia M (1994) Gravel saltation. 2. Modelling. Water Resour Res 30(6):1915–1924
3. Tsuji Y, Morikawa Y, Mizuno O (1985) Experimental measurements of the Magnus force on a rotating sphere at low Reynolds numbers. J Fluid Eng 107:484–488
4. Stokes GG (1843) On some cases of fluid motion. Trans Cambridge Philos Soc 8:105–137
5. Hicks WM (1880) On the motion of two spheres in a fluid. Philos Trans 13:455–492
6. Basset AB (1887) On the motion of two spheres in a liquid, and allied problems. Proc Math Soc 18:369–377
7. Kawaguti M (1964) The flow of a perfect fluid around two moving bodies. J Phys Soc Japan 19:1409–1415
8. Shebalov AN (1967) Unsteady motion of a body under a solid wall or free surface. Mekhanika Zhidkosti i Gaza 2:109–115
9. Kochin NE (1949) O volnovom soprotivlenii i podjemnoj sile pogruzhennyh v zhidkost tel (Wave resistance and lift force of bodies immersed in a liquid). Collected works of N.E. Kochin 2:105–182
10. Voinov OV (1969) O dvizhenii dvukch sfer v idealnoj zhidkosti (On motion of two spheres in ideal liquid). Prikl Mat Mekh 33:659–667
11. Weihs D, Small RD (1975) An exact solution of the motion of two adjacent spheres in axisymmetric potential flow. Israel J Technol 13:1–6
12. Miloh T (1977) Hydrodynamics of deformable contiguous spherical shapes in incompressible inviscid fluid. J Eng Math 11:349–372
13. Bentwich M, Miloh T (1978) On the exact solution for the two-sphere problem in axisymmetrical potential flow. J Appl Mech 45:463–468
14. Yang F-L (2006) Interaction law for a collision between two solid particles in a viscous liquid. PhD thesis, California Institute of Technology. Caltech Library Services. http://etd.caltech.edu/. Cited 26 May 2006
15. Majumder SR (1961) The motion of two spheres in contact parallel to the common line of centres in an incompressible, homogeneous non-viscous fluid. Buletinul Institutului Politehnic din Iasi 7:51–56
16. Small RD, Weihs D (1975) Axisymmetric potential flow over two spheres in contact. J Appl Mech 42:763–765
17. Morrison FA Jr (1976) Irrotational flow about two touching spheres. J Appl Mech 43:365–366

18. Davis AMJ (1977) High frequency limiting virtual-mass coefficients of heaving half-immersed spheres. J Fluid Mech 80:305–319
19. Jeffrey DJ, Chen H-S (1977) The virtual mass of a sphere moving toward a plane wall. J Appl Mech 44:166–167
20. Cox SJ, Cooker MJ (2000) Potential flow past a sphere touching a tangent plane. J Eng Math 38:355–370
21. Odar F, Hamilton WS (1964) Forces on a sphere accelerating in a viscous fluid. J Fluid Mech 18:302–314
22. Shanks D (1955) Nonlinear transformations of divergent and slowly convergent sequences. J Math Phys 34:1–42